JGR Atmospheres

RESEARCH ARTICLE
10.1029/2021JD035776

Special Section:
The Arctic: An AGU Joint Special Collection

The Critical Role of Euro-Atlantic Blocking in Promoting Snowfall in Central Greenland

Claire Pettersen[1,2], Stephanie A. Henderson[3], Kyle S. Mattingly[2], Ralf Bennartz[2,4], and Melissa L. Breeden[5,6]

[1]Climate and Space Sciences and Engineering, University of Michigan, Ann Arbor, MI, USA, [2]Space Science and Engineering Center, University of Wisconsin – Madison, Madison, WI, USA, [3]Department of Atmospheric and Oceanic Sciences, University of Wisconsin – Madison, Madison, WI, USA, [4]Vanderbilt University, Nashville, TN, USA, [5]NOAA Physical Sciences Laboratory, Boulder, CO, USA, [6]Cooperative Institute for Research in the Environmental Sciences, University of Colorado Boulder, Boulder, CO, USA

Abstract The Greenland Ice Sheet (GrIS) is losing mass at an increasing rate yet mass gain from snowfall still exceeds the loss attributed to surface melt processes on an annual basis. This work assesses the relationship between persistent atmospheric blocking across the Euro-Atlantic region and enhanced precipitation processes over the central GrIS during June–August and September–November. Results show that the vast majority of snowfall events in the central GrIS coincide with Euro-Atlantic blocking. During June–August, snowfall events are produced primarily by mixed-phase clouds (88%) and are linked to a persistent blocking anticyclone over southern Greenland (84%). The blocking anticyclone slowly advects warm, moist air masses into western and southern Greenland, with positive temperature and water vapor anomalies that intensify over the central GrIS. A zonal integrated water vapor transport pattern south of Greenland indicates a southern shift of the North Atlantic storm track associated with the high-latitude blocking. In contrast, snowfall events during September–November are largely produced by ice-phase clouds (85%) and are associated with a blocking anticyclone over the Nordic Seas and blocked flow over northern Europe (78%). The blocking anticyclone deflects the westerly North Atlantic storm track poleward and enables the rapid transport of warm, moist air masses up the steep southeastern edge of the GrIS, with positive temperature and water vapor anomalies to the east and southeast of Greenland. These results emphasize the critical role of Euro-Atlantic blocking in promoting snowfall processes over the central GrIS and the importance of accurate representation of blocking in climate model projections.

Plain Language Summary The Greenland Ice Sheet gains mass primarily through snowfall processes. However, the large-scale dynamics leading to snowfall atop the high plateau of central Greenland are not well understood. This study demonstrates that blocking of the mean atmospheric flow by persistent and stationary anticyclones in the Euro-Atlantic region is key in the steering and advection of warm, moist air masses toward central Greenland. Euro-Atlantic blocking is associated with 84% of summer snowfall events over central Greenland and 78% of autumn snowfall events. We find that the location of the blocked flow, the routes of the warm, moist air masses, and the snowfall processes are seasonally dependent. These results emphasize the critical role of Euro-Atlantic blocking in promoting snowfall processes over the central GrIS and the importance of accurate representation of blocking in General Circulation Models.

Key Points:

- The vast majority of enhanced snowfall events observed in central Greenland coincide with Euro-Atlantic blocking
- In summer, snowfall is linked to blocking anticyclones over southern Greenland and the advection of warm, moist air from the west
- In autumn, snowfall is linked to blocking anticyclones in the Nordic Seas, which steer storms toward southeast Greenland

Supporting Information:

Supporting Information may be found in the online version of this article.

Correspondence to:

C. Pettersen,
pettersc@umich.edu

Citation:

Pettersen, C., Henderson, S. A., Mattingly, K. S., Bennartz, R., & Breeden, M. L. (2022). The critical role of Euro-Atlantic blocking in promoting snowfall in central Greenland. *Journal of Geophysical Research: Atmospheres*, *127*, e2021JD035776. https://doi.org/10.1029/2021JD035776

Received 30 AUG 2021
Accepted 28 FEB 2022

Author Contributions:

Conceptualization: Claire Pettersen
Data curation: Claire Pettersen, Stephanie A. Henderson, Kyle S. Mattingly
Formal analysis: Claire Pettersen, Stephanie A. Henderson, Kyle S. Mattingly
Funding acquisition: Ralf Bennartz

1. Introduction

The Greenland Ice Sheet (GrIS) is experiencing an accelerating net loss of mass through melt processes and ice dynamics, contributing to increasing global mean sea level (Mouginot, 2019; van den Broeke, 2016; Zwally et al., 2011). Currently the surface component of the overall GrIS mass balance is positive, as annual snowfall accumulation exceeds mass loss from surface melt processes. GrIS surface mass balance is projected to become negative by the mid-21st century as the atmosphere warms, offsetting projected decreases in glacial discharge (Hofer et al., 2020; Noël et al., 2021). However, the accuracy of these surface mass balance estimates and projections is impeded by uncertainty in snowfall accumulation estimates over the GrIS, with as much as 40% disagreement between various climate and reanalysis model outputs (Cullather et al., 2014), as well as differences between satellite and ground-based observations (Bennartz et al., 2019; McIlhattan et al., 2020). An important contributor to this discrepancy is the intermittent nature of precipitation, as individual storm systems are the major drivers of accumulation in the central GrIS and can be missed by satellite observations which are better suited to capturing

Investigation: Claire Pettersen, Stephanie A. Henderson, Melissa L. Breeden
Methodology: Claire Pettersen, Stephanie A. Henderson
Resources: Claire Pettersen, Ralf Bennartz
Software: Claire Pettersen
Supervision: Claire Pettersen
Validation: Claire Pettersen
Visualization: Claire Pettersen, Stephanie A. Henderson, Kyle S. Mattingly
Writing – original draft: Claire Pettersen, Stephanie A. Henderson
Writing – review & editing: Claire Pettersen, Stephanie A. Henderson, Kyle S. Mattingly, Ralf Bennartz, Melissa L. Breeden

snowfall characteristics at longer time scales (Bennartz et al., 2019; Lenaerts et al., 2020; McIlhattan et al., 2020). Additionally, long-term observations of GrIS precipitation are limited, and many ground sites do not directly measure accumulation (Fausto et al., 2021; Shupe et al., 2013; Steffe & Box, 2001; van As, 2011).

The central plateau of the GrIS is at high elevation (>2,000 m above sea level), is exceptionally dry and cold (Shupe et al., 2013), and experiences a net gain of mass annually (Krabill et al., 2000). The air mass origins and atmospheric dynamical processes that generate precipitation events in the central GrIS are not fully understood, which further contributes to the difficulty in constraining estimates of the surface mass balance (Thomas, 2000). Previous work utilizing ground-based observations atop the GrIS central plateau at Summit Station suggests that clouds (Neff et al., 2014; Solomon & Shupe, 2019) and precipitation (Castellani et al., 2015; Pettersen et al., 2018) are accompanied by anomalously warm, moist southerly air masses. This indicates that understanding the precipitation processes over the central GrIS requires examination of how air masses are transported and modified by weather systems.

Studies focused on enhanced moisture transport to the Arctic have examined impacts and trends on surface temperatures, cloud processes, and sea and land ice (Binder et al., 2017; Neff et al., 2014). Earlier work examining the GrIS illustrated that increased surface melting and a net loss of ice sheet mass is associated with enhanced water vapor transport toward Greenland (Mattingly et al., 2016, 2018). Extratropical cyclones (Dufour et al., 2016; Nygård et al., 2019) as well as Rossby wave breaking (Liu & Barnes, 2015) and the poleward deflection of cyclones (Papritz & Dunn-Sigouin, 2020) are known to transport moisture from the mid-latitudes to the Arctic. Additionally, atmospheric rivers, narrow regions of enhanced horizontal water vapor transport that often form along cold fronts within extratropical cyclones, have been found to be critical in the poleward advection of mid-latitude moisture to the Arctic (Liu & Barnes, 2015; Woods et al., 2013). Consistent among these studies is the importance of highly amplified waves producing substantial poleward excursions of warm, moist air that can reach the GrIS and affect the surface mass balance.

Atmospheric blocks are persistent anticyclones that can significantly disrupt the mean westerly flow both upstream and downstream of the block (Berggren et al., 1949; Rex, 1950), modifying regional precipitation, temperature, and moisture patterns (Henderson et al., 2016; Lenggenhager & Martius, 2019; Masato et al., 2013; Pelly & Hoskins, 2003). Poleward anomalous warm air advection and moisture transport have been found to occur on the western flank of blocking anticyclones (Breeden et al., 2020; Masato et al., 2014; Mundhenk et al., 2016). Additionally, blocks can shift storm tracks latitudinally and steer cyclones poleward (Benedict et al., 2019; Booth et al., 2017; Henderson et al., 2021; Henderson & Maloney, 2018; Pasquier et al., 2019). Investigations specific to the GrIS have largely focused on "Greenland blocks," typically defined using the "Greenland Blocking Index" of mean 500 hPa geopotential height over the spatial region of the GrIS (Hanna et al., 2013). Greenland Blocks are associated with anomalously warm surface temperatures (Hanna et al., 2016; McLeod & Mote, 2016), enhanced water vapor transport (Barrett et al., 2020), and changes in cloud fraction and related surface energy fluxes (Ward et al., 2020), which subsequently affect the surface mass balance of the GrIS. However, studies using the Greenland Blocking Index require the location of the blocking anticyclone to be over Greenland, neglecting impacts from blocking anticyclones over other portions of the Euro-Atlantic region that may also affect the GrIS.

There is currently a need for a comprehensive examination of the relationship between atmospheric blocking over the full Euro-Atlantic region, the poleward advection of anomalous warm, moist air masses, and their subsequent influence on precipitation processes over the GrIS, a critical component of the surface mass balance. General Circulation Models tend to underestimate blocking frequency in the broader Euro-Atlantic region (Masato et al., 2014), and subsequently may misrepresent precipitation processes over Greenland connected to atmospheric blocking. This work examines the relationship between atmospheric blocking over the North Atlantic and Europe and precipitation in the central GrIS during boreal summer and autumn. We find that enhanced precipitation over the central GrIS is associated with atmospheric blocking located over southern Greenland in June, July, August (JJA) and the Nordic Seas in September, October, November (SON). In both seasons, blocking facilitates the northward advection of anomalous warm, moist air masses to the central GrIS.

2. Data and Methods

This work uses observations from the Integrated Characterization of Energy, Clouds, Atmospheric State and Precipitation at Summit (ICECAPS) instrument suite located at Summit Station, Greenland (72°36'N, 38°25'W at 3,216 m above sea level; Shupe et al., 2013). Precipitation events for this study were determined using

observations and methodology from Pettersen et al. (2018). This dataset encompasses observations from June 2010 through February 2017 and has 1-min temporal resolution. Enhanced precipitation events were identified using two key criteria: precipitation must be present for at least 30 min of a given hour (with no requirement that these 30 min are consecutive) and the precipitation rates must be in the uppermost 50% compared to seasonal distributions. The precipitation events are defined by the day and time of onset. Ground-based observations of precipitation occurrence and rate are used to ensure a minimum of 6 hr between the end of an enhanced event and the beginning of another. Methodology from Pettersen et al. (2016, 2018) is used to calculate the associated mean precipitation rate and identify the cloud type for the precipitation events.

The European Centre for Medium-Range Weather Forecasts ERA5 reanalysis products (Hersbach et al., 2020) are used to examine hourly values of 500 hPa winds and geopotential height, 2 m air temperature, 10 m surface wind, and total column water vapor anomaly patterns associated with snowfall events. Additionally, we use the ERA5 vertical integral of eastward water vapor flux and vertical integral of northward water vapor flux to obtain an integrated water vapor transport (IVT) magnitude. Anomalies are calculated by subtracting the historical monthly means (1979–2019) from the respective environmental variable for each individual JJA and SON snowfall event.

Atmospheric blocking is examined for JJA and SON over the North Atlantic and western European region (60°W–40°E) using the ERA-Interim reanalysis (Dee et al., 2011). Blocking frequency is defined following Henderson et al. (2016) and Henderson and Maloney (2018), based on methodology in Masato et al. (2013). This methodology is appropriate as blocking in the Euro-Atlantic region is dominated by dipole-like Rex blocks (e.g., Sousa et al., 2021). A longitude i is considered instantaneously blocked if the integrated 500 hPa geopotential height (Z) north of ϕ_0 latitude is greater than the integrated height to its south, such that $B_i > 0$:

$$B_i = \frac{2}{\Delta\phi}\int_{\phi_0}^{\phi_0+\frac{\Delta\phi}{2}} Z_i\partial\phi - \frac{2}{\Delta\phi}\int_{\phi_0-\frac{\Delta\phi}{2}}^{\phi_0} Z_i\partial\phi \quad (1)$$

Integrations are computed from $\phi_0 = 40°\text{N}–70°\text{N}$, where $\Delta\Phi = 30°$ latitude. See Henderson et al. (2016) for more details. Only large-scale persistent blocking events are examined here, defined when at least 15° of consecutive longitudes are blocked for a minimum of 5 days.

Precipitation events are associated with an atmospheric block if blocking was detected in the defined Atlantic-European region between Day −2 and Day +1 relative to the day of onset of the precipitation event. Day +1 is included since the precipitation event detection method is at hourly resolution while the blocking detection is daily; including Day +1 ensures cases influenced by blocking but with precipitation onset occurring later in the day are included. Additionally, we include Day +1 as the circulation may not quite yet meet the criteria of a large-scale block (e.g., a developing block), but would still impact the circulation that leads to the precipitation event.

A difference of means test was used to determine significance for the precipitation rates associated with and without blocking present and tested at the 95% level. The number of independent events used in calculating significance was determined by events a minimum of 10 days apart to account for the temporal persistence of blocking. A Student's t-test was used to determine regions where geopotential height and temperature anomalies are significantly different from zero at the 95% level. Significance testing of the blocking anomalies was determined using a block bootstrap test as in Henderson et al. (2016). Additionally, the NOAA CPC index of the North Atlantic Oscillation (NAO) was used and no significant relationship to the precipitation events was found for either season.

3. Results

3.1. Seasonal Precipitation and Blocking Characteristics

Ground-based observations are leveraged from the ICECAPS instrument suite to examine precipitation processes over the central GrIS (Pettersen et al., 2016, 2018; Shupe et al., 2013). Currently, precipitation in the central GrIS (>2,000 m ASL) is snowfall (Lenaerts et al., 2020), with the exception of the 14 August 2021 rain event (http://nsidc.org/greenland-today/2021/08/rain-at-the-summit-of-greenland/), and is most frequent and intense during the late boreal summer (JJA) with peak accumulation in August and slowly tapering off throughout autumn (SON) and into winter (Bennartz et al., 2019; Castellani et al., 2015; McIlhattan et al., 2020; Pettersen et al., 2018). In

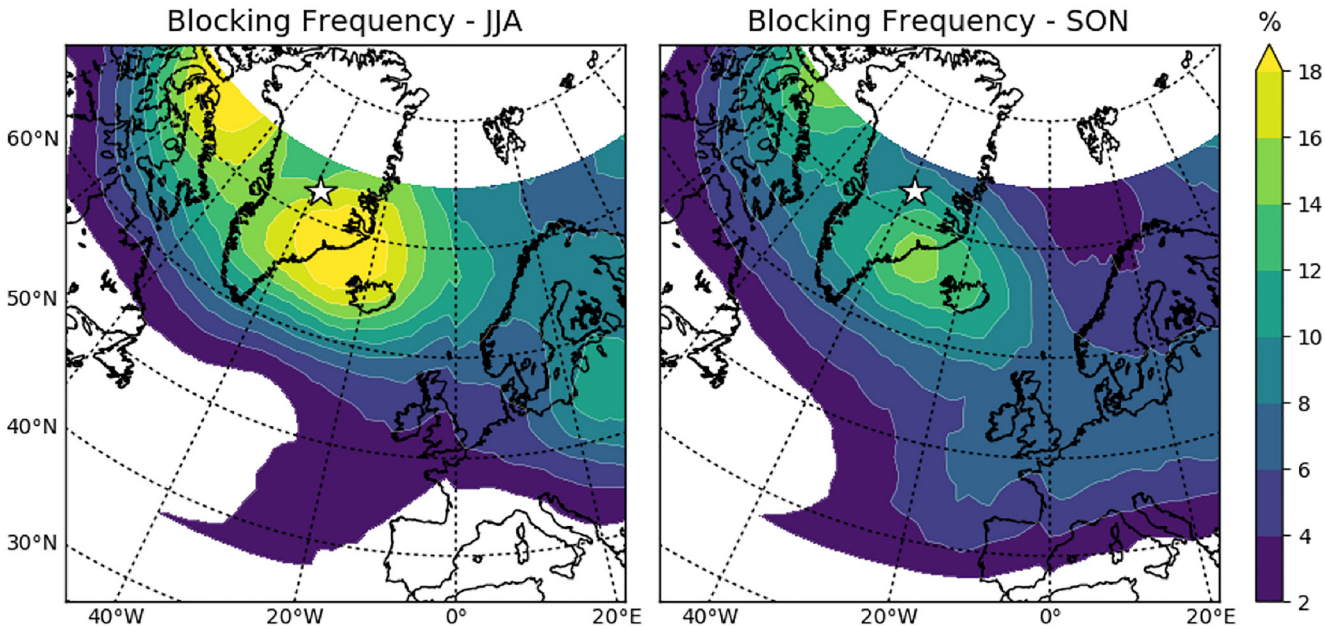

Figure 1. Seasonal climatological blocking frequency means in the Euro-Atlantic region, defined here as 60°W–40°E, 40–70°N, for JJA (a) and SON (b). The blocking frequency index defines a "block" as the blocked region on the southern flank of a persistent large-scale anticyclone, where the associated anomalous easterlies oppose the mean westerlies.

this study we examine enhanced precipitation events, defined as the uppermost 50% snowfall by precipitation rate from 2010 through 2016, and identified 72 events in JJA (Table S1) and 60 events in SON (Table S2).

Using the methodology outlined in Henderson et al. (2016), we track the presence of large-scale (≥15° longitude), persistent (≥5 days) atmospheric blocking throughout a large region of the North Atlantic and Western Europe (blocking maxima between 60°W and 40°E and 35°N to 70°N) for JJA and SON. The mean blocking frequency (1979–2016) in the Euro-Atlantic region illustrates a maximum frequency on the southeast coast of Greenland and into the Denmark Strait for both seasons, though with more frequent blocking in JJA, and a secondary maximum extending into northern Europe (Figure 1). The blocking frequency index used here defines a "block" as the blocked region on the southern flank of a persistent large-scale anticyclone (i.e., a "blocking anticyclone"), where the associated anomalous easterlies oppose the mean westerlies, thereby blocking the mean zonal flow.

We find that between 2 days prior to (Day −2) and 1 day after (Day +1) the onset (Day 0) of snowfall, blocking is present in the defined region during 84% of the JJA and 78% of the SON events. Additionally, snowfall events coincident with an atmospheric block have statistically significantly (see Section 2) higher mean precipitation rates than those events with no blocking present (Table 1). By applying the Pettersen et al. (2018) snow regime classification we found that 88% of the JJA events originated from shallow, mixed-phase clouds (containing supercooled cloud liquid water), while deep, fully glaciated ice-phase clouds produced 85% of the SON events. This is consistent with findings from Pettersen et al. (2018), which showed that precipitation at Summit Station shifts from primarily mixed-phase to ice clouds in late August/early September. The relative difference in precipitation cloud regimes is unsurprising as mixed-phased clouds are often observed over the GrIS during JJA (Shupe

Table 1
Precipitation Event Characteristics by Season

Season	Events	Cloud type	Block (Day −2 to +1)	Mean rate with block	Mean rate without block
JJA	72	88% mixed-phase cloud	84%	0.176 mm hr^{-1}	0.132 mm hr^{-1}
SON	60	85% ice-phase cloud	78%	0.142 mm hr^{-1}	0.121 mm hr^{-1}

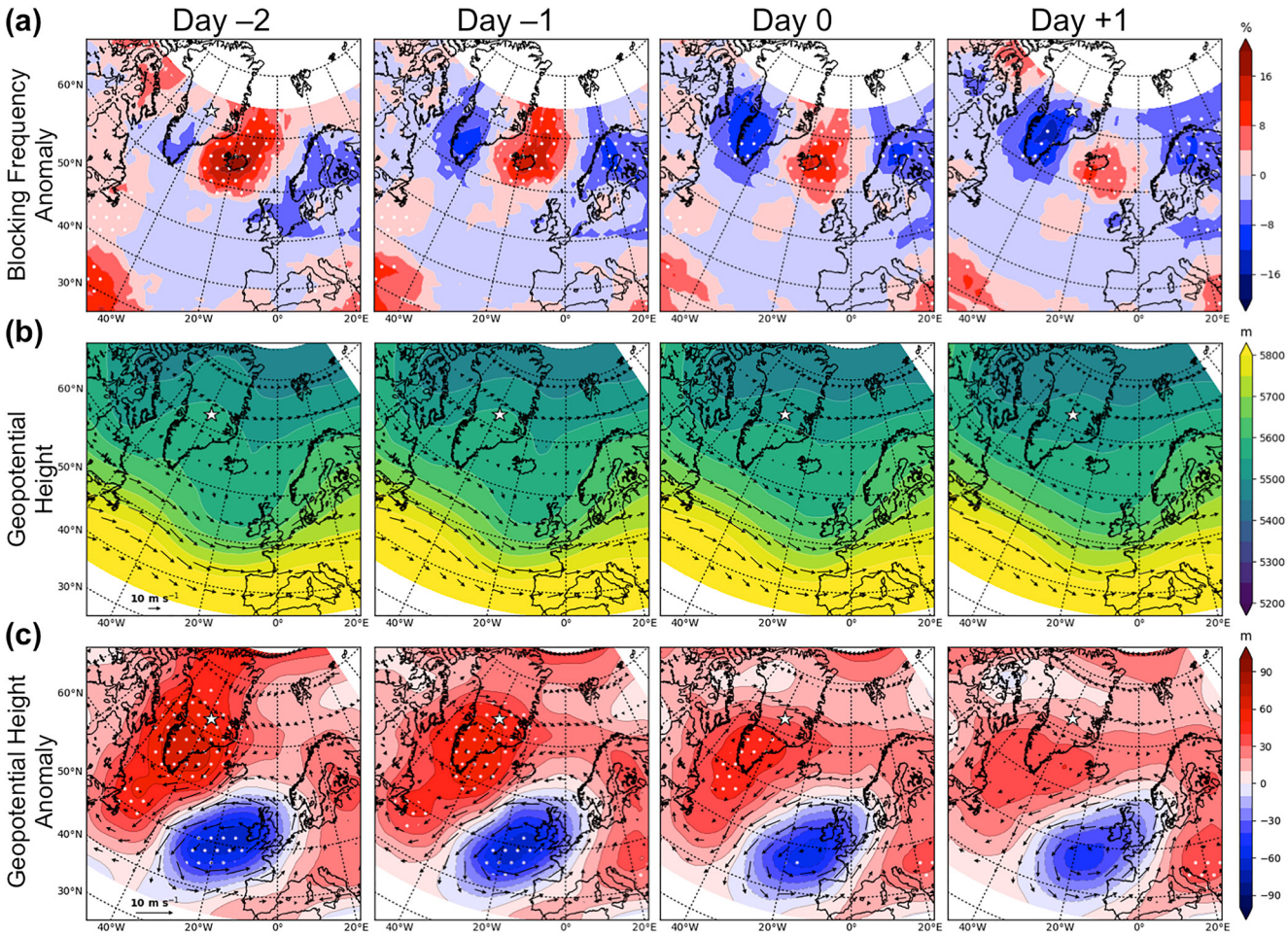

Figure 2. Composites of JJA blocking frequency anomalies (a), 500 hPa geopotential heights and winds (b), and 500 hPa geopotential height and wind anomalies (c) from Day −2 to Day +1 for precipitation events. Blocking frequency anomalies are calculated relative to the JJA seasonal mean (Figure 1). Day 0 indicates the day of precipitation onset at Summit Station. Stippling indicates where anomalies are significant to the 95 percentile.

et al., 2013; van Tricht et al., 2016), whereas deep, synoptically forced precipitation is more common in SON (McIlhattan et al., 2020; Schuenemann et al., 2009).

3.2. JJA Precipitation

The mean meteorological conditions from Day −2 to Day +1 relative to the onset (Day 0) of the 72 individual JJA enhanced snowfall events are illustrated in Figures 2 and 3. During the JJA snowfall events, there is a significant increase in anomalous high-latitude (>60°N) blocking frequency over Iceland (Figure 2a). Blocking is most frequent 2 days prior to precipitation onset (Day −2) and decreases with time through Day +1 (Figure 2a). Additionally, there is a significant reduction of blocking frequency over the southwestern region of the GrIS starting on Day −1 that intensifies through Day +1. The composite of 500 hPa winds also illustrates the blocked flow over Iceland from Day −2 through Day +1 (Figure 2b). The 500 hPa geopotential height shows significant anticyclonic anomalies over the southern GrIS in Day −2 that progressively weaken and become insignificant at Day +1 (Figure 2c). This coincides with anomalous southerly 500 hPa wind components from southwest and west of the GrIS prior to the onset of the JJA snowfall events (Figure 2c).

The high plateau of the central GrIS is extremely cold and dry, and in JJA the average surface temperature ranges from −20°C to −15°C (Shupe et al., 2013). Positive 2 m air temperature anomalies appear off the southern and western coasts of Greenland at Day −2, increasing in the central GrIS prior to the JJA snowfall events and peaking

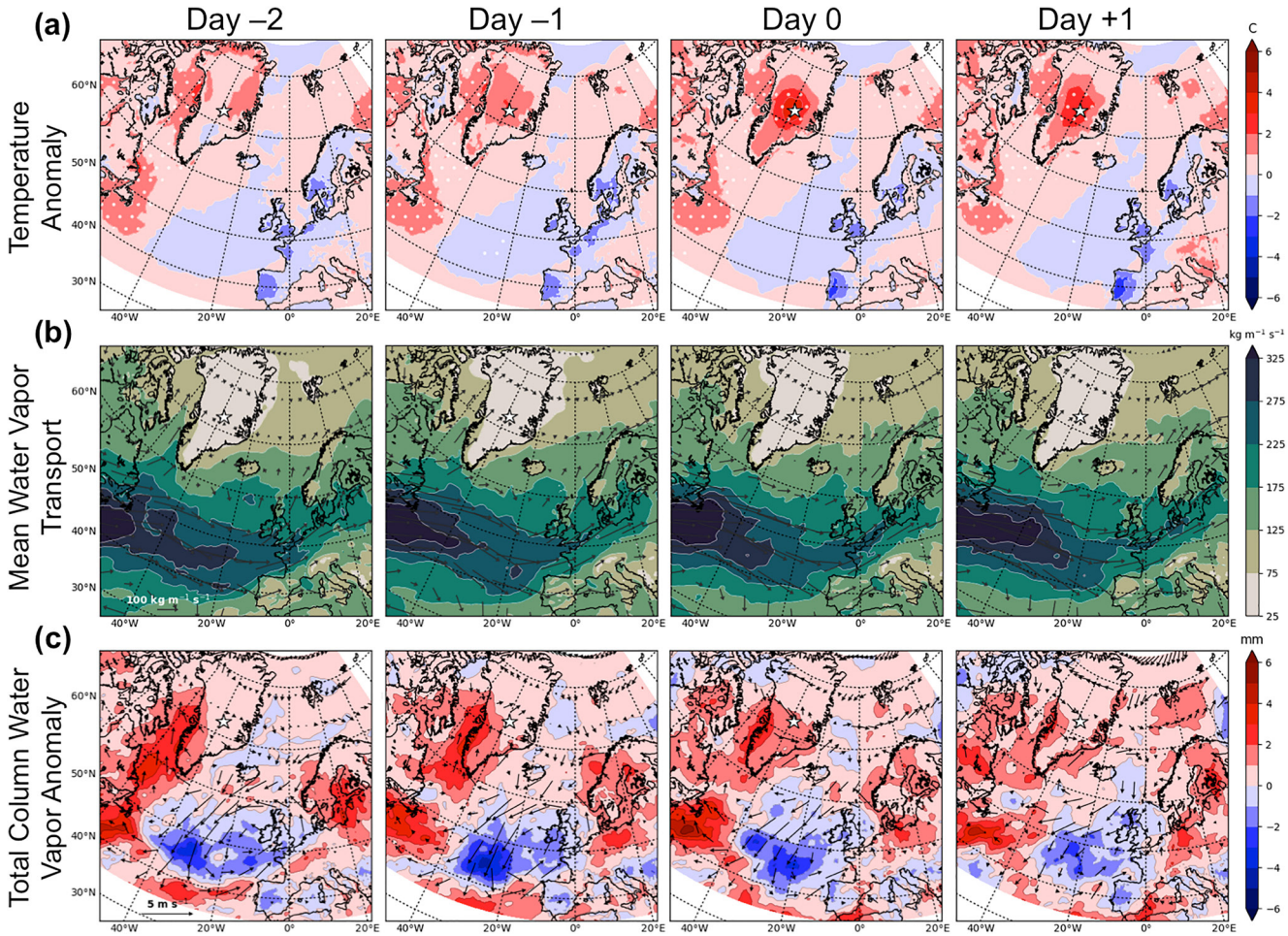

Figure 3. Environmental characteristics from Day −2 to Day +1 for precipitation events during JJA. Composites of 2 m air temperature anomalies (a), water vapor transport and winds (b), and total column water vapor and 10 m wind anomalies (c). Day 0 indicates the day of precipitation onset at Summit Station. Stippling indicates where anomalies are significant to the 95 percentile.

in amplitude on Day 0, with positive temperature anomalies greater than 4°C (Figure 3a). The mean integrated water vapor transport associated with the JJA snowfall events shows enhanced values in the Labrador Sea off the west coast of Greenland peaking at Day −2, and weak southerly mean winds (Figure 3b). The highest values of mean integrated water vapor transport are shifted southward in the region of anomalous blocking frequency between 20°W and 0° longitude when compared to the JJA climatology (not shown). Positive water vapor anomalies (Figure 3c) are observed west of the GrIS (Day −2), and progress from the southwest and west of Greenland up the western slope toward the central GrIS (Day 0), consistent with southerly and southwesterly flow over the western GrIS.

3.3. SON Precipitation

The mean meteorological conditions and anomalies prior to (Day −2) and after (Day +1) the onset of the 60 enhanced snowfall events in SON are exhibited in Figures 4 and 5. The blocking frequency anomalies associated with SON snowfall events illustrate a different evolution, in which significant anomalous blocking of the westerly flow is not observed until Day −1 in the mid-latitudes (50°–60°N) centered over northern Europe (Figure 4a). The composites of 500 hPa winds also indicate blocked flow over northern Europe (Figure 4b). The 500 hPa mean geopotential heights illustrate a blocking anticyclone centered over the North Sea (Figure 4b) and associated anomalies that become significant at Day −1 and continue to amplify (Figure 4c), with a strengthening

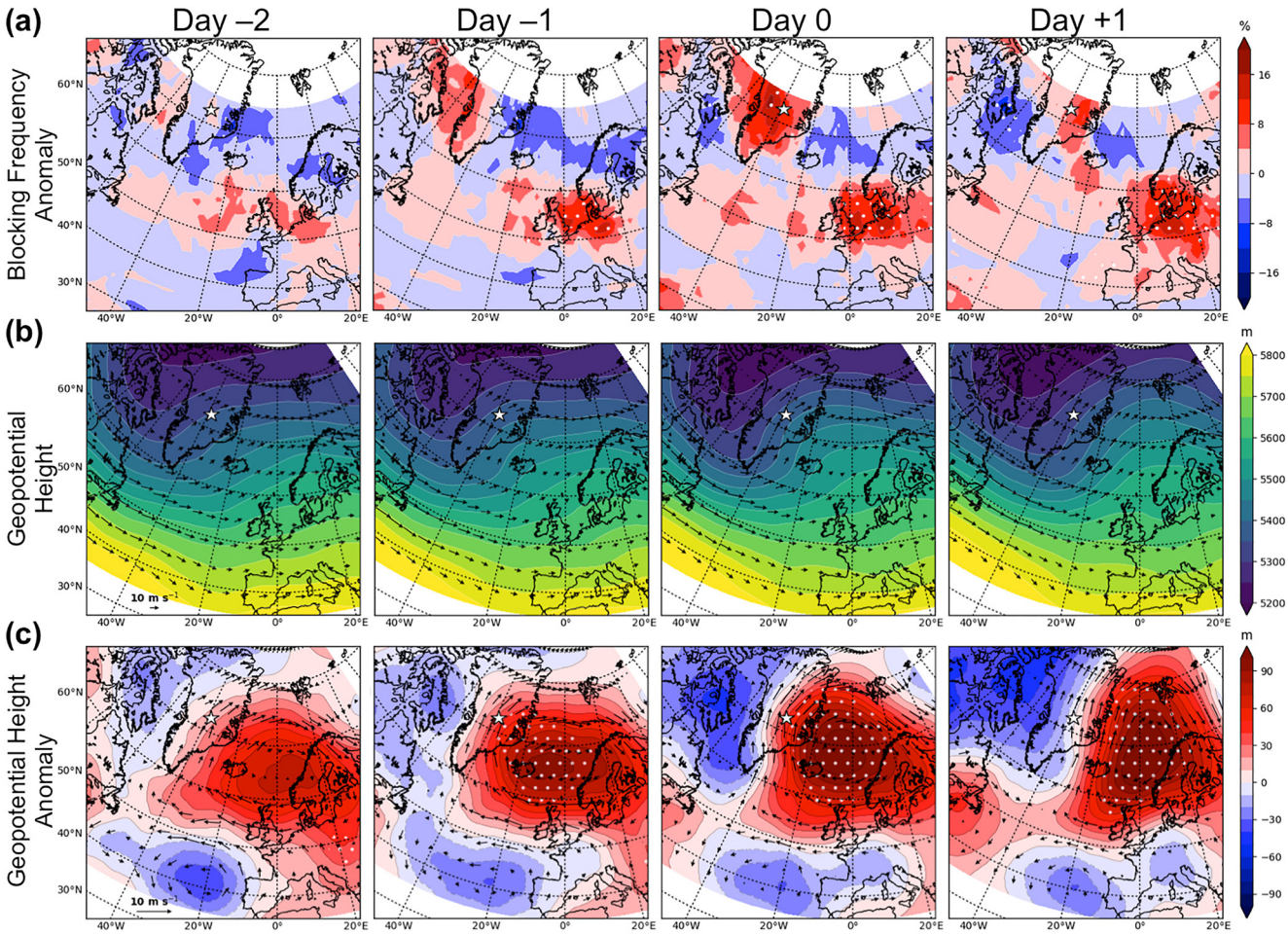

Figure 4. As in Figure 2, but for precipitation events in SON.

height gradient spanning southeast and central Greenland. Anomalous southerly mid-level winds impinge on the southeast coast of the GrIS and strengthen along the western flank of the anticyclone. Just prior to and during snowfall onset, the climatological westerly flow is significantly blocked over northern Europe (Figures 4a and 4b), due to strong opposing easterly wind anomalies along the southern flank of the anomalous blocking anticyclone (Figure 4c). Blocking is also evident west of the anticyclone where a slight reversal of the climatological geopotential height gradient occurs over the GrIS at Day 0.

The central plateau of the GrIS is colder and drier in SON, with average temperatures ranging between −40°C and −20°C (Shupe et al., 2013). During the SON snowfall events, there are significant warm 2 m air temperature anomalies east of Greenland at Day −2 and over the central and southeast GrIS from Day −1 onward (Figure 5a). Positive temperature anomalies are observed west of the blocking anticyclone and strengthen from Day −2 to the onset of snowfall, with values greater than +8°C in the central GrIS at Day 0. At Day +1 there is an indication of the warm temperature anomalies east of the GrIS continuing to propagate northward into the Arctic Ocean. The mean integrated water vapor transport for the SON snowfall events illustrates perturbations in the North Atlantic storm track with strong northward water vapor transport observed along the east coast of Greenland and relatively little zonal transport toward northern Europe (Figure 5b). The water vapor progression during the SON events is shown in Figure 5c, with positive anomalies off the southeast coast of Greenland (Day −2) moving toward the central GrIS (Day 0) and continuing north (Day +1), accompanied by strong southerly surface wind anomalies. The temporal and spatial patterns of the water vapor anomalies and relative location of the blocking frequency anomalies are consistent with the poleward advection of anomalously high values of water vapor along the western flank of the blocking anticyclone.

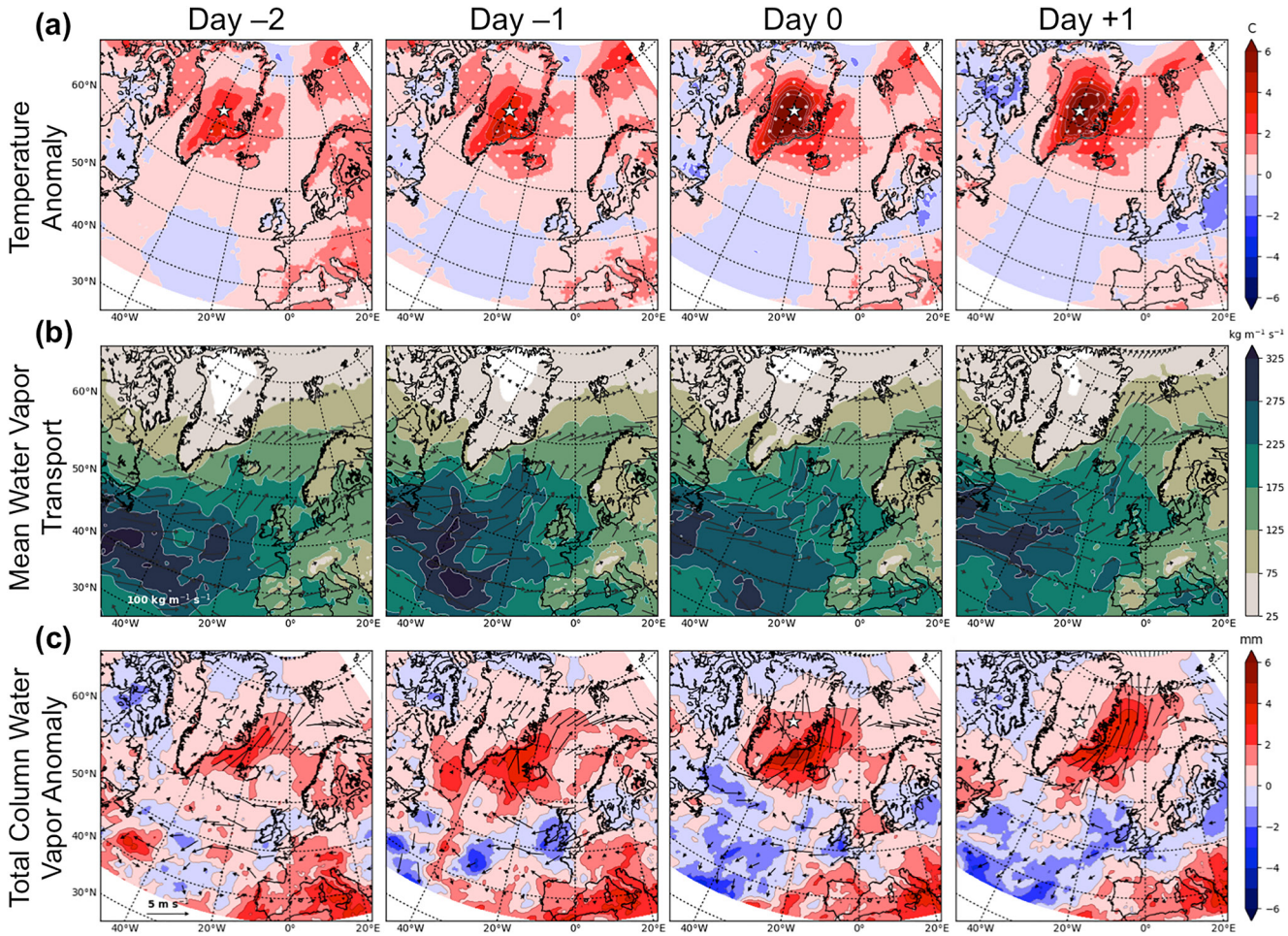

Figure 5. As in Figure 3, but for precipitation events during SON.

4. Discussion

4.1. JJA Precipitation

The blocking frequency anomalies (Figure 2a), and 500 hPa geopotential heights and mid-level winds and anomalies (Figures 2b and 2c) for the JJA snowfall events indicate the advection of air masses primarily from the southwest and west of Greenland. A significant increase in blocking is present as early as 6 days prior to the onset of the JJA snowfall in the central GrIS (not shown). The sustained increase in atmospheric blocking prior to the onset of precipitation may aid in the advection of these slow-moving air masses from south and west of Greenland. Many studies utilize an average of the geopotential height anomaly over the entire GrIS as a measure of Greenland Blocking (e.g., Hanna et al., 2016). However, we find that during JJA snowfall events the significant anomalous anticyclone is located only over the southern GrIS (Figure 2b) and progressively weakens with simultaneous reduced frequency of blocking (Figure 2a). The reduced blocking frequency starting at Day −1 indicates enhanced westerly flow that aids air masses in traversing up the western slope of Greenland toward the central GrIS.

The positive temperature anomalies associated with the JJA snowfall events first develop west of the blocking anticyclone (Figures 2b, 2c and 3a), which is consistent with the poleward advection of warm air masses on the western flanks of atmospheric blocking anticyclones (Breeden et al., 2020; Masato et al., 2014). Additionally, when assessing extreme warming events at Summit Station during JJA in 2012, Neff et al. (2014) found that ridging to the southeast of the GrIS favored the southerly transport of warm air along the western coast of Greenland, similar to the location of the anomalous blocking frequency associated with JJA snowfall events. Previous work

examining the climatological characteristics of Greenland Blocks during JJA found that temperature anomalies over the GrIS correspond to higher 500 hPa geopotential height, with the warmest anomalies located in northern Greenland (McLeod & Mote, 2016). In contrast, we find that at Day −1 the anomalous anticyclone weakens and blocking frequency is decreased while the temperature anomalies continue to increase in the central GrIS along the northern flank of the anticyclonic anomaly, indicating the advection of warm air masses into the region.

The JJA enhanced snow events are associated with high-latitude blocking (Figure 2) and a southward shift in the North Atlantic storm track (Folland et al., 2009), as indicated by the location of the highest values of mean integrated water vapor transport (Figure 3b). This is consistent with previous work that found equatorward shifts in storm tracks during weather regimes with high-latitude blocking (Benedict et al., 2019; Henderson & Maloney, 2018; Pasquier et al., 2019; Woollings et al., 2008). Additionally, there is an indication of increased water vapor transport in the Labrador Sea toward the west coast of Greenland during these events, which is a conduit for mid-latitude moisture transport to the Arctic (Liu & Barnes, 2015; Woods et al., 2013). Furthermore, the poleward advection of anomalously high water vapor values on the western flank of the blocking anticyclone (Figure 3c) is consistent with previous high-latitude blocking studies (e.g., Mundhenk et al., 2016). Earlier work found that anticyclones and Greenland Blocks located over the southeast coast of the GrIS during JJA are associated with enhanced moisture and cloudiness over the west GrIS (Neff et al., 2014; Ward et al., 2020). Additionally, Mattingly et al. (2018) found that while enhanced moisture transport along the west coast of the GrIS during JJA leads to a net loss of mass in the low-elevation ablation zone, the west central GrIS plateau gains mass.

The vast majority (88%) of the JJA snowfall events originate from shallow, mixed-phase clouds. The mid-troposphere characteristics illustrated in Figure 2 imply that there is large-scale flow toward the gentle, western slope of Greenland and onto the central plateau, which is consistent with previous studies that observed a high fraction of precipitating mixed-phase clouds over the west and central GrIS during JJA (McIlhattan et al., 2020; Pettersen et al., 2018). Additionally, the anomalous blocking anticyclone situated over the central and southern GrIS indicates quiescent conditions and weak forcing of vertical motions, which are favorable for sustaining Arctic mixed-phase clouds (Morrison et al., 2012; Shupe et al., 2008). The location of increased blocking frequency during the JJA snowfall events is consistent with the poleward advection of anomalously warm, moist air masses originating from southwest and west of Greenland several days prior to onset. These air masses then travel up the gentle western slope of the GrIS north of the block, aided by a suppressed frequency of blocking and enhanced westerly winds and ultimately producing enhanced snowfall over the central GrIS.

4.2. SON Precipitation

Blocking frequency anomalies associated with SON snowfall events (Figure 4a) and corresponding 500 hPa geopotential heights, winds, and associated anomalies (Figures 4b and 4c) illustrate the rapid transport of air masses southeast of Greenland toward the central GrIS. Positive blocking frequency anomalies emerge over northern Europe at Day −1 as the anticyclonic anomaly in the Nordic Seas amplifies. The development of the blocking anticyclone just prior to the onset of snowfall is consistent with earlier studies of snowfall originating from deep ice-phase clouds, in which trajectory analyses indicate that these air masses move quickly from the southeast coast to the central GrIS, often in less than 12 hr (Pettersen et al., 2018). Additionally, the atmospheric circulation patterns associated with SON events are consistent with those seen for higher snow accumulation in the central plateau of the GrIS (>2,000 m above sea level; Gallagher et al., 2021).

The warm temperature anomalies associated with the SON events (Figure 5a) are located northwest of the blocking anticyclone in the North Sea (Figure 4), which is consistent with the poleward advection of warm air masses on the western flanks of atmospheric blocks (Breeden et al., 2020; Masato et al., 2014). Additionally, the 500 hPa geopotential height and wind anomalies during the SON events (Figure 4c) are similar to circulation patterns corresponding to positive surface temperature anomalies observed in central and southeast Greenland (Gallagher et al., 2020). These warm temperature anomalies continue to propagate northward into the Arctic Ocean (as indicated by the Day +1 panel in Figure 5a), which is identified as a key pathway for the transport of anomalously warm air into the Arctic (Papritz & Dunn-Sigouin, 2020).

The SON enhanced snow events are associated with blocking of the westerly flow in the mid-latitudes (Figure 4) and perturbations in the composite integrated water vapor transport (Figure 5b). These patterns suggest that the North Atlantic storm track is blocked and that storms are rerouted poleward, with distinct northward water vapor

transport toward the GrIS. This is in line with previous studies illustrating that mid-latitude blocking is found to block rather than shift the storm tracks (e.g., Rex, 1950; Woollings et al., 2008; Woollings & Hoskins, 2008). Additionally, in agreement with our results, Woods et al. (2013) found enhanced northward transport of water vapor over the North Atlantic and a poleward deflection of mid-latitude storms when a blocking anticyclone is in the northeast Atlantic basin. Correspondingly, Pasquier et al. (2019) found that blocking over northern Europe led to a poleward shift in the patterns of atmospheric rivers in the North Atlantic. Similar patterns of integrated water vapor transport were found in Berdahl et al. (2018) in association with increased storm track density and intensity on the southeast coast of Greenland, and enhanced wintertime precipitation in the southeast GrIS. Correspondingly, Mattingly et al. (2018) found that enhanced water vapor transport and atmospheric rivers impinging on the southeast coast of Greenland led to increased precipitation in the southeast and central-east plateau of the GrIS.

The SON snowfall events are coincident with predominantly deep, ice-phase clouds (85%), which are produced by large-scale lifting and cyclones affecting the southeast coast of Greenland (McIlhattan et al., 2020; Pettersen et al., 2018; Schuenemann et al., 2009). The strong geopotential height gradient over Greenland upstream of the ridge (Figure 4b) is indicative of upper-level divergence and strong vertical lift, which is necessary to transport the air masses up and over the steep topography and onto the central GrIS, as well as produce clouds and precipitation (Hanna et al., 2006; Holton, 2004; Schuenemann et al., 2009). Additionally, the meridional deflection of the North Atlantic storm track and continued northward advection of anomalously warm and moist air masses (Figure 5) suggest that storms and cyclones are being steered poleward by the mid-latitude blocking of the westerly flow over northern Europe. These storms impinge on the steep topography of southeast Greenland leading to lifting and southerly transport of warm, moist air masses and precipitation to the central GrIS.

5. Summary and Conclusions

This study examines the impacts of atmospheric blocking across the Euro-Atlantic region on precipitation processes over the central GrIS. A two-dimensional blocking methodology, which tracks the reversed meridional height gradient located to the south of blocking anticyclones, was used to identify changes in blocking frequency associated with precipitation over the GrIS. We find that enhanced precipitation in the central GrIS is related to Euro-Atlantic blocking with anomalous blocking present during 84% of JJA and 78% of SON snowfall events. The location and temporal progression of the blocking frequency anomalies are seasonally dependent. JJA snowfall events are linked to a persistent blocking anticyclone over southern Greenland and blocking frequency anomalies centered over Iceland, while SON snowfall events are connected to a rapidly developing blocking anticyclone over the Nordic Seas and blocking frequency anomalies over northern Europe.

JJA enhanced precipitation events are coincident with a persistent blocking anticyclone prior to precipitation onset. The JJA precipitation is primarily produced by Arctic mixed-phase clouds (88%), which can persist in quiescent conditions with slow-moving air masses. There are positive anomalies of 2 m air temperature and water vapor to the west and south of Greenland on the western flank of the blocking anticyclone that intensify over the central GrIS at Day 0. Additionally, there is southerly enhanced water vapor transport into the Labrador Sea and the west coast of Greenland, consistent with studies showing the region to be a conduit for mid-latitude moisture transport to the Arctic that is facilitated by blocking-like atmospheric patterns and Rossby wave breaking (Liu & Barnes, 2015; Naakka et al., 2019). Furthermore, the zonal pattern and southern shift of the highest values of water vapor transport south of Greenland indicate that the North Atlantic storm track may not interact directly with the GrIS during the JJA enhanced precipitation events. The blocking anticyclone acts to advect warm, moist air masses from south and west of Greenland, while a reduction in the frequency of blocking over southern Greenland at Lag −1 coincides with enhanced westerlies aiding in the transportation of the warm, moist air up the relatively gentle slope of Greenland toward the central GrIS.

Enhanced precipitation in SON corresponds to a rapidly developing (Day −1) blocking anticyclone over the Nordic Seas. The majority of the SON precipitation is produced by deep, fully glaciated ice clouds (85%), which are associated with low-pressure disturbances and the associated forcing for ascent. Anomalous positive 2 m air temperature and water vapor to the east and southeast of Greenland is transported along the western flank of the blocking anticyclone, peaking in amplitude over the central GrIS at Day 0. The disruption of zonal water vapor transport shown here indicates that the North Atlantic storm track is blocked and storms are being steered toward the southeast coast of Greenland, directly interacting with the GrIS. This is consistent with studies illustrating

that blocking in the North Atlantic mid-latitudes steers storms poleward (Berdahl et al., 2018; Booth et al., 2017). Additionally, the continued progression of the water vapor anomalies and water vapor transport northward toward the Greenland Sea at Day +1 is consistent with a key pathway through which extratropical cyclones reach the Arctic Ocean (Papritz & Dunn-Sigouin, 2020).

The connection between seasonal Euro-Atlantic blocking and precipitation events in the central GrIS has implications for the surface mass balance of the entire GrIS. The advection of anomalously warm, moist air masses by blocking anticyclones leads to precipitation in the central GrIS and therefore likely a net mass gain. However, the anomalous warm 2 m air temperatures and water vapor transport along the west coast of Greenland in JJA and east coast in SON may lead to a net loss of mass at the margins of the GrIS through both ice sheet melt processes and increased likelihood of rain instead of snowfall at the surface (Niwano et al., 2021). Additionally, the clouds associated with snowfall can impact the surface mass balance. Both the shallow, mixed-phase clouds in JJA and the fully glaciated ice-phase clouds in SON can act to further amplify surface melt processes through radiative effects (Bennartz et al., 2013; Mattingly et al., 2020; van Tricht et al., 2016).

Several studies examining the GrIS find connections between the phase of the North Atlantic Oscillation and increased precipitation (Bromwich et al., 1999) and moisture transport (Sodemann et al., 2008). The influence of the North Atlantic Oscillation on accumulation is found to be most strongly correlated in western Greenland and is spatially variable over the GrIS (Appenzeller et al., 1998; Mosley-Thompson et al., 2005). Recent work indicates that the position of the Icelandic Low with respect to Greenland may be more relevant to enhanced precipitation over the GrIS than the phase of the North Atlantic Oscillation (Auger et al., 2017; Berdahl et al., 2018). In this work, though we found a significant connection to blocking in the Euro-Atlantic region, we found no relationship with the North Atlantic Oscillation for the precipitation in either season. For precipitation events in SON, the water vapor transport is similar to that of Berdahl et al. (2018) and may indicate the importance of the position of the Icelandic Low in promoting storm interaction with southeastern Greenland.

An important implication of this work is the key role of processes that are poorly captured in General Circulation Models, which do not reproduce the recent increasing trend in geopotential heights over Greenland (Delhasse et al., 2021), and tend to underestimate blocking frequency in the broader Euro-Atlantic region (Masato et al., 2014; Schiemann et al., 2017). General Circulation Models also do not produce accurate estimates of snowfall in the central GrIS, potentially due to poorly constrained assumptions from a lack of observations (Lenaerts et al., 2020; Shupe et al., 2013) as well as incorrect assumptions of cloud physics (McIlhattan et al., 2017). Additionally, these models can have biases when dealing with meridional integrated water vapor transport (Espinoza et al., 2018; Waliser & Guan, 2017). This study suggests that in order to accurately model snowfall over Greenland and, in turn, the surface mass balance, atmospheric blocking, moisture transport, cloud type, and precipitation processes must be properly simulated.

Data Availability Statement

The precipitation observations from Summit Station are available in a publicly archived dataset that combines ground-based microwave radiometer, surface precipitation, and meteorological observations (Pettersen & Merrelli, 2018). ERA5 reanalysis data products were used to examine the 500 hPa winds and geopotential height, 2 m air temperature, 10 m surface wind, total column water vapor anomalies, and integrated water vapor fluxes and are publicly available (https://www.ecmwf.int/en/forecasts/datasets/reanalysis-datasets/era5). Atmospheric blocking is determined using 500 hPa geopotential height values from the ERA-Interim reanalysis, which is publicly available (https://www.ecmwf.int/en/forecasts/datasets/reanalysis-datasets/era-interim). Tables of the snow event dates, presence of atmospheric blocking in the Euro-Atlantic region, and associated cloud type are included as comma separated variable files as part of Supporting Information S1 accompanying this manuscript (see Tables S1 and S2).

Acknowledgments
This study is supported by the National Science Foundation Office of Polar Programs Grant Nos. 1801318 and the NOAA Climate and Global Change

References

Appenzeller, C., Schwander, J., Sommer, S., & Stocker, T. F. (1998). The North Atlantic Oscillation and its imprint on precipitation and ice accumulation in Greenland. *Geophysical Research Letters*, *25*, 1939–1942. https://doi.org/10.1029/98gl01227

Auger, J. D., Birkel, S. D., Maasch, K. A., Mayewski, P. A., & Schuenemann, K. C. (2017). Examination of precipitation variability in southern Greenland. *Journal of Geophysical Research: Atmospheres*, *122*, 6202–6216. https://doi.org/10.1002/2016jd026377

Postdoctoral Fellowship Program, administered by UCAR's Cooperative Programs for the Advancement of Earth System Science, under award number NA18NWS4620043B. The authors would like to thank the Summit Station science technicians and staff as well as Polar Field Services for their continued commitment to gathering data and maintaining instrumentation. The authors declare they have no competing interests.

Barrett, B. S., Henderson, G. R., McDonnell, E., Henry, M., & Mote, T. (2020). Extreme Greenland blocking and high-latitude moisture transport. *Atmospheric Science Letters*, *21*, e1002. https://doi.org/10.1002/asl.1002

Benedict, J. J., Clement, A. C., & Medeiros, B. (2019). Atmospheric blocking and other large-scale precursor patterns of landfalling atmospheric rivers in the North Pacific: A CESM2 study. *Journal of Geophysical Research: Atmospheres*, *124*, 11330–11353. https://doi.org/10.1029/2019jd030790

Bennartz, R., Fell, F., Pettersen, C., Shupe, M. D., & Schuettemeyer, D. (2019). Spatial and temporal variability of snowfall over Greenland from CloudSat observations. *Atmospheric Chemistry and Physics*, *19*, 8101–8121. https://doi.org/10.5194/acp-19-8101-2019

Bennartz, R., Shupe, M. D., Turner, D. D., Walden, V. P., Steffen, K., Cox, C. J., et al. (2013). Greenland melt extent enhanced by low-level liquid clouds. *Nature*, *496*, 83–86. https://doi.org/10.1038/nature12002

Berdahl, M., Rennermalm, A., Hammann, A., Mioduszweski, J., Hameed, S., Tedesco, M., et al. (2018). Southeast Greenland winter precipitation strongly linked to the Icelandic low position. *Journal of Climate*, *31*, 4483–4500. https://doi.org/10.1175/jcli-d-17-0622.1

Berggren, R., Bolin, B., & Rossby, C. G. (1949). An aerological study of zonal motion, its perturbations and break-down. *Tellus*, *1*, 14–37. https://doi.org/10.3402/tellusa.v1i2.8501

Binder, H., Boettcher, M., Grams, C. M., Joos, H., Pfahl, S., & Wernli, H. (2017). Exceptional air mass transport and dynamical drivers of an extreme wintertime Arctic warm event. *Geophysical Research Letters*, *44*, 12–028. https://doi.org/10.1002/2017gl075841

Booth, J. F., Dunn-Sigouin, E., & Pfahl, S. (2017). The relationship between extratropical cyclone steering and blocking along the North American East Coast. *Geophysical Research Letters*, *44*, 11–976. https://doi.org/10.1002/2017gl075941

Breeden, M. L., Hoover, B. T., Newman, M., & Vimont, D. J. (2020). Optimal North Pacific blocking precursors and their deterministic subseasonal evolution during Boreal winter. *Monthly Weather Review*, *148*, 739–761. https://doi.org/10.1175/mwr-d-19-0273.1

Bromwich, D. H., Chen, Q. S., Li, Y., & Cullather, R. I. (1999). Precipitation over Greenland and its relation to the North Atlantic Oscillation. *Journal of Geophysical Research: Atmospheres*, *104*, 22103–22115. https://doi.org/10.1029/1999jd900373

Castellani, B. B., Shupe, M. D., Hudak, D. R., & Sheppard, B. E. (2015). The annual cycle of snowfall at Summit, Greenland. *Journal of Geophysical Research: Atmospheres*, *120*, 6654–6668. https://doi.org/10.1002/2015jd023072

Cullather, R. I., Nowicki, S. M., Zhao, B., & Suarez, M. J. (2014). Evaluation of the surface representation of the Greenland Ice Sheet in a general circulation model. *Journal of Climate*, *27*, 4835–4856. https://doi.org/10.1175/jcli-d-13-00635.1

Dee, D. P., Uppala, S. M., Simmons, A. J., Berrisford, P., Poli, P., Kobayashi, S., et al. (2011). The ERA-Interim reanalysis: Configuration and performance of the data assimilation system. *Quarterly Journal of the Royal Meteorological Society*, *137*, 553–597. https://doi.org/10.1002/qj.828

Delhasse, A., Hanna, E., Kittel, C., & Fettweis, X. (2021). Brief communication: CMIP6 does not suggest any atmospheric blocking increase in summer over Greenland by 2100. *International Journal of Climatology*, *41*, 2589–2596. https://doi.org/10.1002/joc.6977

Dufour, A., Zolina, O., & Gulev, S. K. (2016). Atmospheric moisture transport to the Arctic: Assessment of reanalyses and analysis of transport components. *Journal of Climate*, *29*, 5061–5081. https://doi.org/10.1175/jcli-d-15-0559.1

Espinoza, V., Waliser, D. E., Guan, B., Lavers, D. A., & Ralph, F. M. (2018). Global analysis of climate change projection effects on atmospheric rivers. *Geophysical Research Letters*, *45*, 4299–4308. https://doi.org/10.1029/2017gl076968

Fausto, R. S., van As, D., Mankoff, K. D., Vandecrux, B., Citterio, M., Ahlstrøm, A. P., et al. (2021). Programme for monitoring of the Greenland Ice Sheet (PROMICE) automatic weather station data. *Earth System Science Data*, *13*, 3819–3845. https://doi.org/10.5194/essd-13-3819-2021

Folland, C. K., Knight, J., Linderholm, H. W., Fereday, D., Ineson, S., & Hurrell, J. W. (2009). The summer North Atlantic Oscillation: Past, present, and future. *Journal of Climate*, *22*, 1082–1103. https://doi.org/10.1175/2008jcli2459.1

Gallagher, M., Shupe, M., Chepfer, H., & L'Ecuyer, T. (2021). Relating snowfall observations to Greenland ice sheet mass changes: An atmospheric circulation perspective. *The Cryosphere Discussions*, 1–26. https://doi.org/10.5194/tc-16-435-2022

Gallagher, M. R., Chepfer, H., Shupe, M. D., & Guzman, R. (2020). Warm temperature extremes across Greenland connected to clouds. *Geophysical Research Letters*, *47*, e2019GL086059. https://doi.org/10.1029/2019gl086059

Hanna, E., Cropper, T. E., Hall, R. J., & Cappelen, J. (2016). Greenland blocking index 1851–2015: A regional climate change signal. *International Journal of Climatology*, *36*, 4847–4861. https://doi.org/10.1002/joc.4673

Hanna, E., Jones, J. M., Cappelen, J., Mernild, S. H., Wood, L., Steffen, K., & Huybrechts, P. (2013). The influence of North Atlantic atmospheric and oceanic forcing effects on 1900–2010 Greenland summer climate and ice melt/runoff. *International Journal of Climatology*, *33*, 862–880. https://doi.org/10.1002/joc.3475

Hanna, E., McConnell, J., Das, S., Cappelen, J., & Stephens, A. (2006). Observed and modeled Greenland ice sheet snow accumulation, 1958–2003, and links with regional climate forcing. *Journal of Climate*, *19*, 344–358. https://doi.org/10.1175/jcli3615.1

Henderson, G. R., Barrett, B. S., Wachowicz, L. J., Mattingly, K. S., Preece, J. R., & Mote, T. L. (2021). Local and remote atmospheric circulation drivers of Arctic change: A review. *Frontiers of Earth Science*, *9*, 549. https://doi.org/10.3389/feart.2021.709896

Henderson, S. A., & Maloney, E. D. (2018). The impact of the Madden–Julian oscillation on high-latitude winter blocking during El Niño–Southern Oscillation events. *Journal of Climate*, *31*, 5293–5318. https://doi.org/10.1175/jcli-d-17-0721.1

Henderson, S. A., Maloney, E. D., & Barnes, E. A. (2016). The influence of the Madden–Julian oscillation on Northern Hemisphere winter blocking. *Journal of Climate*, *29*, 4597–4616. https://doi.org/10.1175/jcli-d-15-0502.1

Hersbach, H., Bell, B., Berrisford, P., Hirahara, S., Horányi, A., Muñoz-Sabater, J., et al. (2020). The ERA5 global reanalysis. *Quarterly Journal of the Royal Meteorological Society*, *146*, 1999–2049. https://doi.org/10.1002/qj.3803

Hofer, S., Lang, C., Amory, C., Kittel, C., Delhasse, A., Tedstone, A., & Fettweis, X. (2020). Greater Greenland Ice Sheet contribution to global sea level rise in CMIP6. *Nature Communications*, *11*, 1–11. https://doi.org/10.1038/s41467-020-20011-8

Holton, J. (2004). *An introduction to dynamical meteorology* (4th ed., pp. 151–155).

Krabill, W., Abdalati, W., Frederick, E., Manizade, S., Martin, C., Sonntag, J., et al. (2000). Greenland ice sheet: High-elevation balance and peripheral thinning. *Science*, *289*, 428–430. https://doi.org/10.1126/science.289.5478.428

Lenaerts, J., Camron, M. D., Wyburn-Powell, C. R., & Kay, J. E. (2020). Present-day and future Greenland Ice Sheet precipitation frequency from CloudSat observations and the Community Earth system model. *The Cryosphere*, *14*, 2253–2265. https://doi.org/10.5194/tc-14-2253-2020

Lenggenhager, S., & Martius, O. (2019). Atmospheric blocks modulate the odds of heavy precipitation events in Europe. *Climate Dynamics*, *53*, 4155–4171. https://doi.org/10.1007/s00382-019-04779-0

Liu, C., & Barnes, E. A. (2015). Extreme moisture transport into the Arctic linked to Rossby wave breaking. *Journal of Geophysical Research: Atmospheres*, *120*, 3774–3788. https://doi.org/10.1002/2014jd022796

Masato, G., Hoskins, B. J., & Woollings, T. J. (2013). Winter and summer Northern Hemisphere blocking in CMIP5 models. *Journal of Climate*, *26*, 7044–7059. https://doi.org/10.1175/jcli-d-12-00466.1

Masato, G., Woollings, T., & Hoskins, B. J. (2014). Structure and impact of atmospheric blocking over the Euro-Atlantic region in present-day and future simulations. *Geophysical Research Letters*, *41*, 1051–1058. https://doi.org/10.1002/2013gl058570

Mattingly, K. S., Mote, T. L., & Fettweis, X. (2018). Atmospheric river impacts on Greenland Ice Sheet surface mass balance. *Journal of Geophysical Research: Atmospheres*, *123*, 8538–8560. https://doi.org/10.1029/2018jd028714

Mattingly, K. S., Mote, T. L., Fettweis, X., Van As, D., Van Tricht, K., Lhermitte, S., et al. (2020). Strong summer atmospheric rivers trigger Greenland Ice Sheet melt through spatially varying surface energy balance and cloud regimes. *Journal of Climate*, *33*, 6809–6832. https://doi.org/10.1175/jcli-d-19-0835.1

Mattingly, K. S., Ramseyer, C. A., Rosen, J. J., Mote, T. L., & Muthyala, R. (2016). Increasing water vapor transport to the Greenland Ice Sheet revealed using self-organizing maps. *Geophysical Research Letters*, *43*, 9250–9258. https://doi.org/10.1002/2016gl070424

McIlhattan, E. A., L'Ecuyer, T. S., & Miller, N. B. (2017). Observational evidence linking Arctic supercooled liquid cloud biases in CESM to snowfall processes. *Journal of Climate*, *30*, 4477–4495. https://doi.org/10.1175/jcli-d-16-0666.1

McIlhattan, E. A., Pettersen, C., Wood, N. B., & L'Ecuyer, T. S. (2020). Satellite observations of snowfall regimes over the Greenland Ice Sheet. *The Cryosphere*, *14*, 4379–4404. https://doi.org/10.5194/tc-14-4379-2020

McLeod, J. T., & Mote, T. L. (2016). Linking interannual variability in extreme Greenland blocking episodes to the recent increase in summer melting across the Greenland ice sheet. *International Journal of Climatology*, *36*, 1484–1499. https://doi.org/10.1002/joc.4440

Morrison, H., De Boer, G., Feingold, G., Harrington, J., Shupe, M. D., & Sulia, K. (2012). Resilience of persistent Arctic mixed-phase clouds. *Nature Geoscience*, *5*, 11–17. https://doi.org/10.1038/ngeo1332

Mosley-Thompson, E., Readinger, C. R., Craigmile, P., Thompson, L. G., & Calder, C. A. (2005). Regional sensitivity of Greenland precipitation to NAO variability. *Geophysical Research Letters*, *32*. https://doi.org/10.1029/2005gl024776

Mouginot, J., Rignot, E., Bjørk, A. A., van den Broeke, M., Millan, R., Morlighem, M., et al. (2019). Forty-six years of Greenland Ice Sheet mass balance from 1972 to 2018. *Proceedings of the National Academy of Sciences of the United States of America*, *116*, 9239–9244. https://doi.org/10.1073/pnas.1904242116

Mundhenk, B. D., Barnes, E. A., Maloney, E. D., & Nardi, K. M. (2016). Modulation of atmospheric rivers near Alaska and the US West Coast by northeast Pacific height anomalies. *Journal of Geophysical Research: Atmospheres*, *121*, 12–751. https://doi.org/10.1002/2016jd025350

Naakka, T., Nygård, T., Vihma, T., Sedlar, J., & Graversen, R. (2019). Atmospheric moisture transport between mid-latitudes and the Arctic: Regional, seasonal and vertical distributions. *International Journal of Climatology*, *39*, 2862–2879. https://doi.org/10.1002/joc.5988

Neff, W., Compo, G. P., Martin Ralph, F., & Shupe, M. D. (2014). Continental heat anomalies and the extreme melting of the Greenland ice surface in 2012 and 1889. *Journal of Geophysical Research: Atmospheres*, *119*, 6520–6536. https://doi.org/10.1002/2014jd021470

Niwano, M., Box, J. E., Wehrlé, A., Vandecrux, B., Colgan, W. T., & Cappelen, J. (2021). Rainfall on the Greenland Ice Sheet: Present-day climatology from a high-resolution non-hydrostatic polar regional climate model. *Geophysical Research Letters*, *48*, e2021GL092942. https://doi.org/10.1029/2021gl092942

Noël, B., van Kampenhout, L., Lenaerts, J. T. M., van de Berg, W. J., & Van Den Broeke, M. R. (2021). A 21st century warming threshold for sustained Greenland Ice Sheet mass loss. *Geophysical Research Letters*, *48*, e2020GL090471.

Nygård, T., Graversen, R. G., Uotila, P., Naakka, T., & Vihma, T. (2019). Strong dependence of wintertime Arctic moisture and cloud distributions on atmospheric large-scale circulation. *Journal of Climate*, *32*, 8771–8790.

Papritz, L., & Dunn-Sigouin, E. (2020). What configuration of the atmospheric circulation drives extreme net and total moisture transport into the Arctic. *Geophysical Research Letters*, *47*, e2020GL089769. https://doi.org/10.1029/2020gl089769

Pasquier, J. T., Pfahl, S., & Grams, C. M. (2019). Modulation of atmospheric river occurrence and associated precipitation extremes in the North Atlantic region by European weather regimes. *Geophysical Research Letters*, *46*, 1014–1023. https://doi.org/10.1029/2018gl081194

Pelly, J. L., & Hoskins, B. J. (2003). A new perspective on blocking. *Journal of Atmospheric Science*, *60*, 743–755. https://doi.org/10.1175/1520-0469(2003)060<0743:anpob>2.0.co;2

Pettersen, C., Bennartz, R., Kulie, M. S., Merrelli, A. J., Shupe, M. D., & Turner, D. D. (2016). Microwave signatures of ice hydrometeors from ground-based observations above Summit, Greenland. *Atmospheric Chemistry and Physics*, *16*, 4743–4756. https://doi.org/10.5194/acp-16-4743-2016

Pettersen, C., Bennartz, R., Merrelli, A. J., Shupe, M. D., Turner, D. D., & Walden, V. P. (2018). Precipitation regimes over central Greenland inferred from 5 years of ICECAPS observations. *Atmospheric Chemistry and Physics*, *18*, 4715–4735. https://doi.org/10.5194/acp-18-4715-2018

Pettersen, C., & Merrelli, A. J. (2018). *Microwave radiometer snow categorization tool for Summit, Greenland, 2010 – 2015*. Arctic Data Center. https://doi.org/10.18739/A2R28Q

Rex, D. F. (1950). Blocking action in the middle troposphere and its effect upon regional climate. *Tellus*, *2*, 275–301. https://doi.org/10.3402/tellusa.v2i4.8603

Schiemann, R., Demory, M. E., Shaffrey, L. C., Strachan, J., Vidale, P. L., Mizielinski, M. S., et al. (2017). The resolution sensitivity of Northern Hemisphere blocking in four 25-km atmospheric global circulation models. *Journal of Climate*, *30*, 337–358. https://doi.org/10.1175/jcli-d-16-0100.1

Schuenemann, K. C., Cassano, J. J., & Finnis, J. (2009). Synoptic forcing of precipitation over Greenland: Climatology for 1961–99. *Journal of Hydrometerology*, *10*, 60–78. https://doi.org/10.1175/2008jhm1014.1

Shupe, M. D., Daniel, J. S., De Boer, G., Eloranta, E. W., Kollias, P., Long, C. N., et al. (2008). A focus on mixed-phase clouds: The status of ground-based observational methods. *Bulletin of the American Meteorological Society*, *89*, 1549–1562. https://doi.org/10.1175/2008bams2378.1

Shupe, M. D., Turner, D. D., Walden, V. P., Bennartz, R., Cadeddu, M. P., Castellani, B. B., et al. (2013). High and dry: New observations of tropospheric and cloud properties above the Greenland Ice Sheet. *Bulletin of the American Meteorological Society*, *94*, 169–186. https://doi.org/10.1175/bams-d-11-00249.1

Sodemann, H., Masson-Delmotte, V., Schwierz, C., Vinther, B. M., & Wernli, H. (2008). Interannual variability of Greenland winter precipitation sources: 2. Effects of North Atlantic Oscillation variability on stable isotopes in precipitation. *Journal of Geophysical Research: Atmospheres*, *113*, D12. https://doi.org/10.1029/2007jd009416

Solomon, A., & Shupe, M. D. (2019). A case study of airmass transformation and cloud formation at Summit, Greenland. *Journal of Atmospheric Science*, *76*, 3095–3113. https://doi.org/10.1175/jas-d-19-0056.1

Sousa, P. M., Barriopedro, D., García-Herrera, R., Woollings, T., & Trigo, R. M. (2021). A new combined detection algorithm for blocking and subtropical ridges. *Journal of Climate*, *34*, 7735–7758. https://doi.org/10.1175/jcli-d-20-0658.1

Steffe, K., & Box, J. (2001). Surface climatology of the Greenland ice sheet: Greenland climate network 1995–1999. *Journal of Geophysical Research: Atmospheres*, *106*, 33951–33964. https://doi.org/10.1029/2001jd900161

Thomas, R. H. E. A., Akins, T., Csatho, B., Fahnestock, M., Gogineni, P., Kim, C., & Sonntag, J. (2000). Mass balance of the Greenland Ice Sheet at high elevations. *Science*, *289*, 426–428. https://doi.org/10.1126/science.289.5478.426

van As, D. (2011). Programme for monitoring of the Greenland Ice Sheet (PROMICE): First temperature and ablation records. *Geological Survey of Denmark and Greenland Bulletin*, *23*, 73–76.

van den Broeke, M. R., Enderlin, E. M., Howat, I. M., Kuipers Munneke, P., Noël, B. P. Y., van de Berg, W. J., et al. (2016). On the recent contribution of the Greenland ice sheet to sea level change. *The Cryosphere*, *10*, 1933–1946. https://doi.org/10.5194/tc-10-1933-2016

van Tricht, K., Lhermitte, S., Lenaerts, J. T., Gorodetskaya, I. V., L'Ecuyer, T. S., Noël, B., et al. (2016). Clouds enhance Greenland ice sheet meltwater runoff. *Nature Communications*, *7*, 1–9. https://doi.org/10.1038/ncomms10266

Waliser, D., & Guan, B. (2017). Extreme winds and precipitation during landfall of atmospheric rivers. *Nature Geoscience*, *10*, 179–183. https://doi.org/10.1038/ngeo2894

Ward, J. L., Flanner, M. G., & Dunn-Sigouin, E. (2020). Impacts of Greenland block location on clouds and surface energy fluxes over the Greenland Ice Sheet. *Journal of Geophysical Research: Atmospheres*, *125*, e2020JD033172. https://doi.org/10.1029/2020jd033172

Woods, C., Caballero, R., & Svensson, G. (2013). Large-scale circulation associated with moisture intrusions into the Arctic during winter. *Geophysical Research Letters*, *40*, 4717–4721. https://doi.org/10.1002/grl.50912

Woollings, T., & Hoskins, B. (2008). Simultaneous Atlantic–Pacific blocking and the northern annular mode. *Quarterly Journal of the Royal Meteorological Society*, *134*, 1635–1646. https://doi.org/10.1002/qj.310

Woollings, T., Hoskins, B., Blackburn, M., & Berrisford, P. (2008). A new Rossby wave–breaking interpretation of the North Atlantic Oscillation. *Journal of Atmospheric Science*, *65*, 609–626. https://doi.org/10.1175/2007jas2347.1

Zwally, H. J., Li, J., Brenner, A. C., Beckley, M., Cornejo, H. G., DiMarzio, J., et al. (2011). Greenland ice sheet mass balance: Distribution of increased mass loss with climate warming; 2003–07 versus 1992–2002. *Journal of Glaciology*, *57*, 88–102. https://doi.org/10.3189/002214311795306682